2014

Thermodynamic Assessment of High-Temperature Heat Pumps for Heat Recovery

Chieko Kondou
Kyushu University, Japan, kondo.chieko.162@m.kyushu-u.ac.jp

Shigeru Koyama
Kyushu University, Japan, koyama@cm.kyushu-u.ac.jp

Thermodynamic Assessment of High-Temperature Heat Pumps for Heat Recovery

Chieko KONDOU[1]*, Shigeru KOYAMA[1, 2]

[1] Kyushu University, Interdisciplinary Graduate School of Engineering Science, Fukuoka, Japan
E-mail; kondo.chieko.162@m.kyushu-u.ac.jp

[2] Kyushu University, International Institute for Carbon-Neutral Energy Research, Fukuoka, Japan
E-mail; koyama@phase.cm.kyushu-u.ac.jp

ABSTRACT

Reducing energy consumption by utilizing heat recovery systems has become increasingly important in industry. For this problem, heat pumps are one solution to recover waste heat. This paper presents an exploratory assessment of heat pump-type heat recovery systems using environmentally friendly refrigerants. The coefficient of performance (COP) of four different cycle configurations used to raise the temperature of heat media up to 160 °C with a waste heat of 80 °C are calculated and compared for the refrigerants R717, R365mfc, R1234ze(E), and R1234ze(Z). A multiple-stage "extraction" cycle drastically reduces the throttling loss in the expansion valve and the exergy loss in the condensers and consequently achieves the highest COP among the calculated cases with R1234ze(Z). A cascade cycle using R1234ze(Z) and R365mfc has a relatively high COP and also provides many practical benefits. Even with adverse conditions, the primary energy efficiency is greater than 1.3 when the transmission-end efficiency of the electric power generation is 0.37. The thermodynamic assessment demonstrated that the use of high-temperature heat pumps to recover waste heat is promising to reduce primary energy consumption for industrial applications.

1. INTRODUCTION

Steam boilers are often used for the drying process of wood or paint, food processing, the distillation process of drugs or drinks, and the cleaning process of machined components. However, in boiler systems, the heat loss from the large steam pipe and the emissions of greenhouse gases from fossil fuel consumption are considerable. Additionally, the heat exhaust from these relatively high-temperature processes is not utilized in many cases (e.g., US DOE, 2003). Therefore, recently, an attempt to introduce industrial heat pumps to recover waste heat and reduce primary energy consumption has attracted attention (e.g., US DOE, 2008; Jacobs et al., 2010). Conversely, in the past, there was a view that the efficiency of a heat pump is inferior to combustion in primary energy conversion (Kew, 1982). From the above significance, this study provides a brief thermodynamic assessment as the first screening of refrigerants and a case study to calculate more specifically the performances of proposed cycle configurations. First, a theoretical coefficient of performance (COP) of a basic heating cycle at condensing temperatures from 50 °C to the critical temperatures are evaluated for several refrigerants. Based on this screening, candidate refrigerants with different levels of critical temperature are selected, and four different cycle configurations are proposed for a case study. Secondly, the COP and the primary energy efficiency of these cycles using the selected refrigerants are calculated for the case of raising temperature of compressed water as a heat media up to 160 °C with waste heat of 80 °C. From the calculation results, the characteristic of the proposed cycles and the optimum refrigerant for the target temperature are discussed in this paper.

2. THEORETICAL PERFORMANCE OF SELECTED REFRIGERANTS

Table 1 compares the characteristics and properties of the selected refrigerants for industrial high-temperature heat pumps. In Table 1, the refrigerants are listed in the order of their critical temperature from left to right. The gray columns are newly recognized substances as refrigerants; the white columns are conventional refrigerants. The low GWP refrigerant R1234ze(E) and the isomer R1234ze(Z) have been vigorously investigated in this decade (Brown et al. 2009) as alternatives to R134a and R245fa. The natural refrigerant R717, i.e., ammonia, has excellent thermodynamic properties, as mentioned by many forerunners (e.g., Fleming, 1978; Pearson, 1999), and also quite strong toxicity. R717 is, therefore, considered only for the non-usage or low-pressure side in this study. R365 has the highest critical temperature among the selected refrigerants. Although R365mfc has a relatively high GWP, a low-GWP alternative with similar physical properties, such as HFEs, will likely be found shortly.

Figure 1 shows the performance of a theoretical heat-pump cycle using the selected refrigerants. Figure 1 (a) illustrates the calculation conditions of a theoretical cycle on the refrigerant *T-s* diagram to evaluate the heating COP, COP_H, pressure ratio, P_d/P_s, and volumetric capacity, VC_H. The temperature lift of 80 K and the subcool of 60 K are rather larger than the typical operation conditions of air conditioners and simulate an operation for the industrial heat pumps for waste heat recovery. The physical properties are calculated using REFPROP 9.1 (Lemmon et al., 2010) coupled with the incorporated coefficients optimized by Akasaka et al. (2013). Under the given conditions, the COP_H and VC_H are defined as below.

$$COP_H = \Delta h_{cond} / \Delta h_{compr} \ , \quad \text{and} \quad VC_H = \rho_V \Delta h_{cond} \tag{1}$$

In Figures 1 (b), (c), and (d), COP_H, P_d/P_s, and VC_H are, respectively, plotted by varying the condensation temperature from 50 to the temperature just below the critical point. As the condensation temperature rises to the critical temperature, the COP monotonically increases. This theoretical COP indicates the possible line of the developments and does not take account of the irreversible losses. The pressure ratio decreases with increasing temperature, whereas the volumetric capacity increases. Under the condition of such a large temperature lift of 80 K, the pressure ratio easily exceeds 5. Operating steadily at pressure ratios beyond 5 with a single compression is difficult with existing technology. When the volumetric capacity is insufficient or far smaller than that of

Table 1: Fundamental characteristics of candidate refrigerants

	R410A	R134a	R1234ze(E)	R717	R1234ze(Z)	R245fa	R365mfc
ODP	0	0	0	0	0	0	0
GWP_{100}*	6	1430	6	negligible	<10	1030	794
Safety classification**	A1	A1	A2L	B2	A2L*** (expected)	B1	A2 (expected)
NBP**** [°C]	-51.5	-26.1	-19.0	-33.3	9.8	15.1	40.2
P_{crit} [MPa]	4.90	4.06	3.64	11.33	3.53	3.65	3.27
T_{crit} [°C]	71.3	101.1	109.4	132.3	150.1	154.0	186.9

* IPCC 4th report (Solomon et al., 2007) ** ANSI/ASHRAE standard 34-2007 (A-Non-toxic, B-Toxic; 1-Non-flammable, 1L-Mildly flammable, 2-Flammable) *** Koyama et al. (2012) **** Normal boiling point

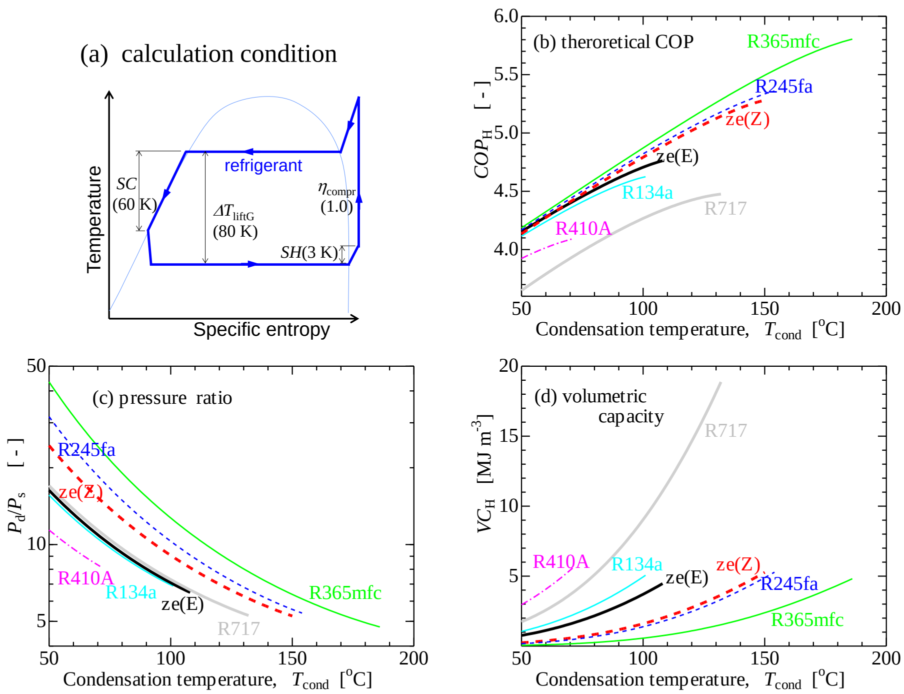

Figure 1: Theoretical COP of a basic heating cycle allows large subcooling for selected refrigerants (ΔT_{liftG} = 80 K, SC = 60 K, SH = 3 K, η_{compr}= 1.0). The notations “ze(E)” and “ze(Z)” refer R1234ze(E) and R1234ze(Z), respectively.

conventional refrigerants, to maintain the heating capacity with same size of compressor and heat exchangers, the irreversible loss is prone to increase due to the required much higher refrigerant circulation ratio. To avoid this problem, much larger equipment is required; however, the market would not accept such an economic burden. To reduce the pressure ratio while increasing the volumetric capacity, techniques of multiple stages or cascading would be necessary, and selecting a refrigerant to operate at just below the critical temperature at a given condition is also important. Based upon this brief assessment, a case study with more specific cycle configurations on a heat recovery system is hereafter discussed.

3. CASE STUDY ON HEAT RECOVERY SYSTEMS TO RAISE TEMPERATURE FROM 80 TO 160 °C

In the following case study, the performance of an industrial heat pump system to recover waste heat is calculated. Utilizing the waste heat of 80 ˚C, the heat media of compressed water is preheated to 75 ˚C. Then, the compressed water at 1 MPa is heated from 75 ˚C to 160 ˚C by a heat pump system and delivers the heat to the usage site. The waste heat is, of course, used as the heat source of the heat pump.

3.1 Cycle configurations

Figure 2 shows four cycle configurations of the heat pump system for heat recovery. Figures 2 (a), (b), (c), and (d) are the proposed cycles: a triple tandem cycle, a two stage extraction cycle, a three stage extraction cycle, and a cascade cycle. In the triple tandem cycle of Figure 2 (a), an internal heat exchanger is used to reduce the pressure ratio of the third cycle. The extraction cycle shown in Figures 2 (b) and (c) is a unique system to extract the vapor from the compressor. The extracted vapor rejects heat in a condenser and then converges with the liquid that flowed through a condenser and an expansion valve on the higher pressure side. After the conversion, the enthalpy and the mass flow rate are increased by the liquid from the higher pressure side, and the heat is rejected to the compressed water in a sub-cooler. By converging the extracted vapor and the liquid from the higher-pressure side, the internal energy remaining in the liquid is utilized in the sub-cooler instead of losing it as the throttling loss in an expansion valve returning to the evaporator. In the cascade cycle of Figure 2 (d), the compressed water is heated with a sub-cooler of the low temperature side cycle and continuously heated in the two stage extraction cycle of the high temperature side cycle. In the case where the COP is improved, an internal heat exchanger is applied in the cycles of Figures 2 (c) and (d), as drawn by the dashed line. The above cycles are stated as cases I, II, III, and IV in this paper.

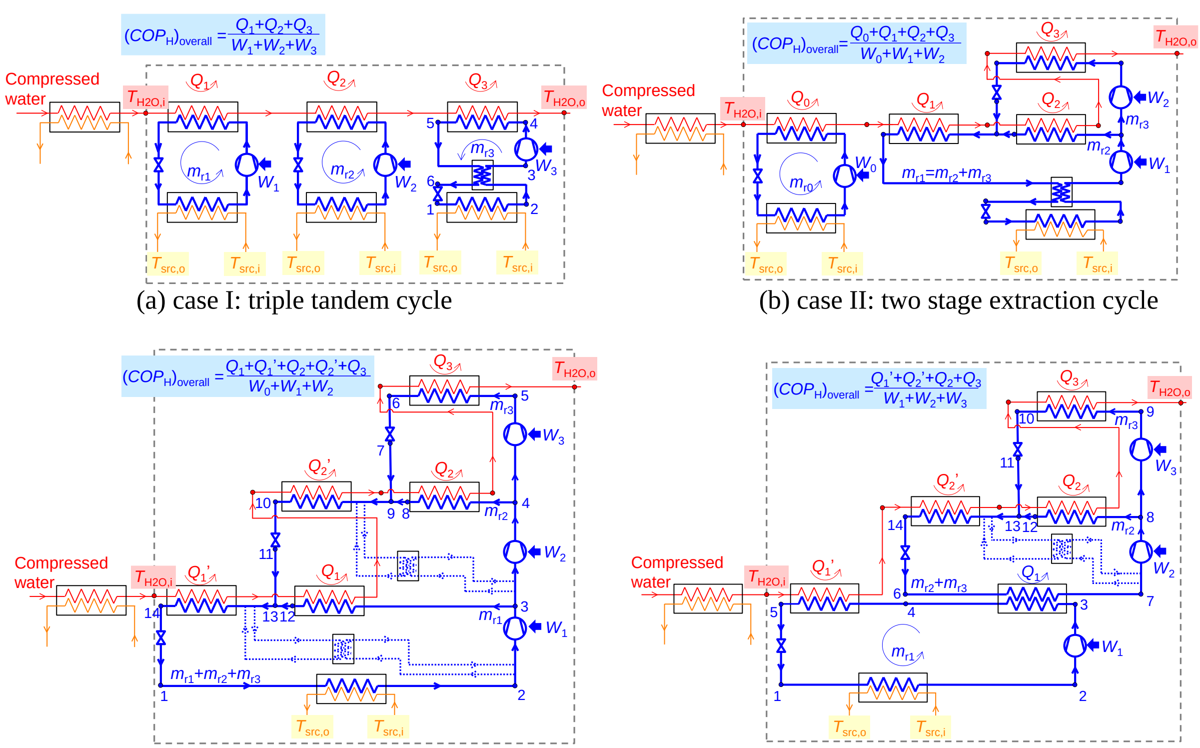

(a) case I: triple tandem cycle

(b) case II: two stage extraction cycle

(c) case III: three stage extraction cycle

(d) case IV: cascade cycle

Figure 2: Proposed cycle configurations for the heat recovery system

3.2 Calculation conditions and models for components

Compressor: Regardless of the pressure ratio or the rotation speed, the isentropic, mechanical, and motor efficiency are given as 0.92, 0.85, and 0.90 for each compressor or compression process.

Evaporator: Figure 3 illustrates the calculation model of the temperature distribution in the evaporator and the condenser/gas-cooler/subcooler on the *T-Q* diagram of the refrigerant. In this model, the pinch temperature (i.e., minimum approach temperature) is 5 K in the subcool and superheat regions, whereas it is 2 K in the two-phase region. The evaporation pressure is a saturation pressure that corresponds to the saturation temperature that is 2 K below the outlet temperature of the heat source fluid. The outlet temperature of superheated vapor is 5 K below the inlet temperature of the heat source fluid.

Condenser/Gas-cooler/Subcooler: As shown in Figure 3, the condensation pressure is determined as corresponding to a saturation temperature that is 2 K above the outlet temperature of the compressed water. In the case where the pressure exceeds the critical point, the pressure in the gas-cooler is determined with a pinch temperature of 5 K. The gas-cooler is partitioned into 10 segments on the basis of entropy change, and the pinch temperature is the minimum temperature difference in those segments. For the subcooler, the pinch point that appears either at the entrance or the exit is greater than 5 K.

Internal heat exchanger: As drawn by the dotted lines in Figure 2, an internal heat exchanger can be taken into account if it improves COP or if it is necessary to keep the refrigerant state superheated at the compressor discharge. The pinch point at either the entrance or the exit is always greater than 2 K. Under these conditions, the optimum point of the compressor suction temperature and the heat transfer rate in the internal heat exchanger are iteratively found.

3.3 Calculation procedure for case III and IV

The coefficient of performance (COP) of case III is calculated as follows. Considering the efficiencies, the shaft power $\Delta h_{\mathrm{compr}}$ and the total energy consumption W of compressors are expressed as,

$$\begin{cases} \Delta h_{\mathrm{compr1}} = \left[h_{\mathrm{r3}}\left(P_3, s_2\right) - h_{\mathrm{r2}}\right] / \left(\eta_s \eta_{\mathrm{mech}}\right) \\ \Delta h_{\mathrm{compr2}} = \left[h_{\mathrm{r8}}\left(P_8, s_7\right) - h_{\mathrm{r7}}\right] / \left(\eta_s \eta_{\mathrm{mech}}\right) \\ \Delta h_{\mathrm{compr3}} = \left[h_{\mathrm{r9}}\left(P_9, s_8\right) - h_{\mathrm{r8}}\right] / \left(\eta_s \eta_{\mathrm{mech}}\right) \end{cases} \quad \begin{cases} W_1 = \left(\Delta h_{\mathrm{compr1}} \eta_{\mathrm{motor}}\right) m_{\mathrm{r1}} \\ W_2 = \left(\Delta h_{\mathrm{compr2}} \eta_{\mathrm{motor}}\right)\left(m_{\mathrm{r2}} + m_{\mathrm{r3}}\right) \\ W_3 = \left(\Delta h_{\mathrm{compr3}} \eta_{\mathrm{motor}}\right) m_{\mathrm{r3}} \end{cases} \tag{2}$$

When the inlet temperatures of the compressed water in the heat exchangers 2’ and 3 of heat transfer rates Q_2’and Q_3 are given, the state of this cycle is determined to satisfy the following heat balances.

$$\begin{cases} Q_1' = \left[h_{\mathrm{H2O}}\left(T_{\mathrm{H2O,i}}^{\mathrm{cond1}}\right) - h_{\mathrm{H2O}}\left(T_{\mathrm{H2O,i}}\right)\right] m_{\mathrm{H2O}} = \left(h_{\mathrm{r14}} - h_{\mathrm{r13}}\right)\left(m_{\mathrm{r3}} + m_{\mathrm{r2}} + m_{\mathrm{r1}}\right) \\ Q_1 = \left[h_{\mathrm{H2O}}\left(T_{\mathrm{H2O,i}}^{\mathrm{cond2'}}\right) - h_{\mathrm{H2O}}\left(T_{\mathrm{H2O,i}}^{\mathrm{cond1}}\right)\right] m_{\mathrm{H2O}} = \left(h_{\mathrm{r3}} - h_{\mathrm{r12}}\right) m_{\mathrm{r1}} \\ Q_2' = \left[h_{\mathrm{H2O}}\left(T_{\mathrm{H2O,i}}^{\mathrm{cond2}}\right) - h_{\mathrm{H2O}}\left(T_{\mathrm{H2O,i}}^{\mathrm{cond2'}}\right)\right] m_{\mathrm{H2O}} = \left(h_{\mathrm{r9}} - h_{\mathrm{r10}}\right)\left(m_{\mathrm{r3}} + m_{\mathrm{r2}}\right) \\ Q_2 = \left[h_{\mathrm{H2O}}\left(T_{\mathrm{H2O,i}}^{\mathrm{cond3}}\right) - h_{\mathrm{H2O}}\left(T_{\mathrm{H2O,i}}^{\mathrm{cond2}}\right)\right] m_{\mathrm{H2O}} = \left(h_{\mathrm{r4}} - h_{\mathrm{r8}}\right) m_{\mathrm{r2}} \\ Q_3 = \left[h_{\mathrm{H2O}}\left(T_{\mathrm{H2O,o}}\right) - h_{\mathrm{H2O}}\left(T_{\mathrm{H2O,i}}^{\mathrm{cond3}}\right)\right] m_{\mathrm{H2O}} = \left(h_{\mathrm{r5}} - h_{\mathrm{r6}}\right) m_{\mathrm{r3}} \end{cases} \tag{3}$$

With a given heat load (Q_1’+Q_1+Q_2’+Q_2+Q_3) and the compressed water temperatures $T_{\mathrm{H2O,i}}^{\mathrm{cond2'}}$ and $T_{\mathrm{H2O,i}}^{\mathrm{cond3}}$, the remaining

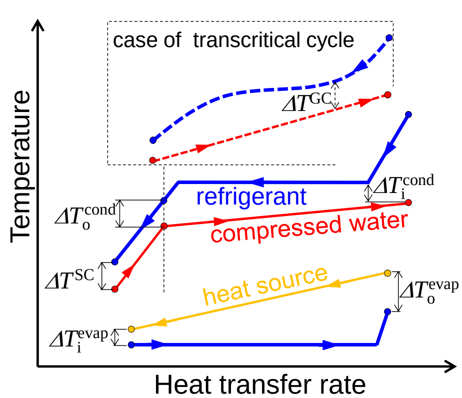

Figure 3: Model for the approach temperature and pinch points in the heat exchangers

Table 2: Typical calculation conditions for the case study

Compressed water (1 MPa)	inlet temp. (after pre-heating)	$T_{\mathrm{H2O,i}}$	70°C
	outlet temp.	$T_{\mathrm{H2O,o}}$	160°C
Heat source	inlet temp.	$T_{\mathrm{src,i}}$	80°C
	outlet temp.	$T_{\mathrm{src,o}}$	70°C
Compressor	isentropic efficiency	η_{s}	0.92
	mechanical efficiency	η_{mech}	0.85
	motor efficiency	η_{motor}	0.90
Evaporator	pinch temp. at the entrance	$\Delta T_{\mathrm{i}}^{\mathrm{evap}}$	> 2 K
	pinch temp. at the exit	$\Delta T_{\mathrm{o}}^{\mathrm{evap}}$	> 5 K
Condenser	pinch temp. at the entrance	$\Delta T_{\mathrm{i}}^{\mathrm{cond}}$	> 2 K
	pinch temp. at the exit	$\Delta T_{\mathrm{o}}^{\mathrm{cond}}$	> 5 K
Gas-cooler	pinch temp.	ΔT^{GC}	> 5 K
Subcooler	pinch temp.	ΔT^{SC}	> 5 K
Internal HEX	pinch temp.	ΔT^{IH}	> 2 K

compressed water temperature $T_{\mathrm{H2O,i}}^{\mathrm{cond1}}$ and the refrigerant mass flow rates m_{r1}, m_{r2}, and m_{r3} are iteratively obtained. Thus, the overall COP of the heating cycle of case III is,

$$\left(COP_{\mathrm{H}}\right)_{\mathrm{overall}} = \frac{Q_1' + Q_1 + Q_2' + Q_2 + Q_3}{W_1 + W_2 + W_3} \tag{4}$$

For the cascade cycle case IV, the shaft power $\Delta h_{\mathrm{compr}}$ and the energy consumption W in the compressors are,

$$\begin{cases} \Delta h_{\mathrm{compr1}} = \left[h_{\mathrm{r3}}\left(P_3, s_2\right) - h_{\mathrm{r2}}\right] / \left(\eta_s \eta_{\mathrm{mech}}\right) \\ \Delta h_{\mathrm{compr2}} = \left[h_{\mathrm{r8}}\left(P_8, s_7\right) - h_{\mathrm{r7}}\right] / \left(\eta_s \eta_{\mathrm{mech}}\right) \\ \Delta h_{\mathrm{compr3}} = \left[h_{\mathrm{r9}}\left(P_9, s_8\right) - h_{\mathrm{r8}}\right] / \left(\eta_s \eta_{\mathrm{mech}}\right) \end{cases} \quad \begin{cases} W_1 = \left(\Delta h_{\mathrm{compr1}} \eta_{\mathrm{motor}}\right) m_{\mathrm{r1}} \\ W_2 = \left(\Delta h_{\mathrm{compr2}} \eta_{\mathrm{motor}}\right)\left(m_{\mathrm{r2}} + m_{\mathrm{r3}}\right) \\ W_3 = \left(\Delta h_{\mathrm{compr3}} \eta_{\mathrm{motor}}\right) m_{\mathrm{r3}} \end{cases} \tag{5}$$

The cycle state is determined when the inlet temperatures of the compressed water in the heat exchangers 2’ and 3, $T_{\mathrm{H2O,i}}^{\mathrm{cond2'}}$ and $T_{\mathrm{H2O,i}}^{\mathrm{cond3}}$, are given to satisfy the following heat balances.

$$\begin{cases} Q_1' = \left[h_{\mathrm{H2O}}\left(T_{\mathrm{H2O,i}}^{\mathrm{cond1}}\right) - h_{\mathrm{H2O}}\left(T_{\mathrm{H2O,i}}\right)\right] m_{\mathrm{H2O}} = \left(h_{\mathrm{r4}} - h_{\mathrm{r5}}\right) m_{\mathrm{r1}} \\ Q_2' = \left[h_{\mathrm{H2O}}\left(T_{\mathrm{H2O,i}}^{\mathrm{cond2}}\right) - h_{\mathrm{H2O}}\left(T_{\mathrm{H2O,i}}^{\mathrm{cond2'}}\right)\right] m_{\mathrm{H2O}} = \left(h_{\mathrm{r13}} - h_{\mathrm{r14}}\right)\left(m_{\mathrm{r3}} + m_{\mathrm{r2}}\right) \\ Q_2 = \left[h_{\mathrm{H2O}}\left(T_{\mathrm{H2O,i}}^{\mathrm{cond3}}\right) - h_{\mathrm{H2O}}\left(T_{\mathrm{H2O,i}}^{\mathrm{cond2}}\right)\right] m_{\mathrm{H2O}} = \left(h_{\mathrm{r8}} - h_{\mathrm{r12}}\right) m_{\mathrm{r2}} \\ Q_3 = \left[h_{\mathrm{H2O}}\left(T_{\mathrm{H2O,o}}\right) - h_{\mathrm{H2O}}\left(T_{\mathrm{H2O,i}}^{\mathrm{cond3}}\right)\right] m_{\mathrm{H2O}} = \left(h_{\mathrm{r9}} - h_{\mathrm{r10}}\right) m_{\mathrm{r3}} \end{cases} \tag{6}$$

Additionally, in the cascade condenser, the following heat balance is maintained.

$$Q_1 = \left(h_{\mathrm{r3}} - h_{\mathrm{r4}}\right) m_{\mathrm{r1}} = \left(h_{\mathrm{r7}} - h_{\mathrm{r6}}\right)\left(m_{\mathrm{r2}} + m_{\mathrm{r3}}\right) \tag{7}$$

From the above conditions, the refrigerant mass flow rates are determined at a given heat load. Thus, the overall COP of the heating cycle of case IV is,

$$\left(COP_{\mathrm{H}}\right)_{\mathrm{overall}} = \frac{Q_1' + Q_2' + Q_2 + Q_3}{W_1 + W_2 + W_3} \tag{8}$$

By sequentially varying the parameters $T_{\mathrm{H2O,i}}^{\mathrm{cond2'}}$ and $T_{\mathrm{H2O,i}}^{\mathrm{cond3}}$, the combinations to maximize the overall COP of Eqs. (4) and (8) are found for case III and case IV.

3.4 Calculation results for the target temperature of 160 °C with the typical conditions

Table 3 lists the calculation results of the overall COP and supplementary information: the change in the compressed water temperature, refrigerants, COP, volumetric capacity, pressure ratio of the individual value or name for each stage. The performance is also expressed in terms of the primary energy efficiency, assuming the transmission-end-efficiency of electric power generation of 0.37. As listed in Table 3, all of the primary energy efficiencies are above 1.0, which indicates positive perspectives for the reduction of the primary energy consumption by the heat pump heat recovery systems. Figures 4, 5, and 6 are *P-h* and *T-s* diagrams that show the calculation results for the high-temperature heat pump cycles of case I, III, and IV, respectively. The thick solid line indicates the state of the refrigerant along with numbers corresponding to those in Figure 2. The other two thin solid lines in the *T-s* diagrams indicate the temperature of the compressed water and heat source fluid as addressed to the refrigerant state. It should be noted that the horizontal axis shows the specific entropy of the refrigerant but not the water or heat source fluid. The temperatures of the compressed water and heat source correspond to the refrigerant state.

Figure 4 plots the results of the triple tandem cycle applying R1234ze(E), R1234ze(Z), and R365mfc for low, medium, and high sides, respectively. The major concern is the large pressure ratio of the high side cycle. In consequence of the large throttling loss due to the pressure ratio beyond 8, the overall COP decreases. To reduce the throttling loss, a momentum recovery using an ejector or an expander could be a possible solution. This would be a necessary step in the development, although this cycle has the advantage of easy control by the independent stages.

Cases II and III of the multiple stage extraction cycle achieve much higher COP than that of the tandem cycle. When R1234ze(Z) and R365mfc are applied in the two stage extraction cycle (case II), as listed in Table 3, the overall COP is 4.83. When either R1234ze(Z) or R365mfc is applied in the three stage extraction cycle (case III-a or III-b), the COP is 4.94 or 4.84. Especially for the three stage extraction cycle, the pressure ratio of each stage is reduced

Table 3: Calculation results for the supply temperature of 160 ˚C with a heat source temperature of 80 ˚C

<table>
<tr><td rowspan="5">case</td><td colspan="2">$T_{H2O}1$</td><td colspan="2">$T_{H2O}2$</td><td colspan="2">$T_{H2O}3$</td><td rowspan="5">overall COP, $(COP_H)_{overall}$</td><td rowspan="5">primary energy efficiency, η_{pe}*</td></tr>
<tr><td colspan="2">refrig.1</td><td colspan="2">refrig.2</td><td colspan="2">refrig.3</td></tr>
<tr><td colspan="2">COP1</td><td colspan="2">COP2</td><td colspan="2">COP3</td></tr>
<tr><td colspan="2">VC1</td><td colspan="2">VC2</td><td colspan="2">VC3</td></tr>
<tr><td colspan="2">P_d/P_s1</td><td colspan="2">P_d/P_s2</td><td colspan="2">P_d/P_s3</td></tr>
<tr><td rowspan="5">I</td><td colspan="2">70 to 100</td><td colspan="2">100 to 130</td><td colspan="2">130 to 160</td><td rowspan="5">4.37</td><td rowspan="5">1.62</td></tr>
<tr><td colspan="2">R1234ze(E)</td><td colspan="2">R1234ze(Z)</td><td colspan="2">R365mfc</td></tr>
<tr><td colspan="2">7.88</td><td colspan="2">4.14</td><td colspan="2">3.15</td></tr>
<tr><td colspan="2">11.54</td><td colspan="2">4.80</td><td colspan="2">2.32</td></tr>
<tr><td colspan="2">2.04</td><td colspan="2">4.01</td><td colspan="2">8.43</td></tr>
<tr><td rowspan="5">II</td><td colspan="2">70 to 90</td><td colspan="2">90 to 129</td><td colspan="2">129 to 160</td><td rowspan="5">4.83</td><td rowspan="5">1.79</td></tr>
<tr><td colspan="3">R1234ze(Z)</td><td colspan="3">R365mfc</td></tr>
<tr><td colspan="3">10.96</td><td colspan="3">4.18</td></tr>
<tr><td colspan="3">5.56</td><td colspan="3">-</td></tr>
<tr><td colspan="2">1.77</td><td colspan="2">4.66</td><td colspan="2">1.81</td></tr>
<tr><td rowspan="5">III-a</td><td colspan="2">70 to 99</td><td colspan="2">99 to 125</td><td colspan="2">125 to 160</td><td rowspan="5">4.94</td><td rowspan="5">1.83</td></tr>
<tr><td colspan="6">R1234ze(Z)</td></tr>
<tr><td colspan="6">4.94</td></tr>
<tr><td colspan="6">-</td></tr>
<tr><td colspan="2">2.16</td><td colspan="2">1.69</td><td colspan="2">1.62</td></tr>
<tr><td rowspan="5">III-b</td><td colspan="2">70 to 104</td><td colspan="2">104 to 128</td><td colspan="2">128 to 160</td><td rowspan="5">4.84</td><td rowspan="5">1.79</td></tr>
<tr><td colspan="6">R365mfc</td></tr>
<tr><td colspan="6">4.84</td></tr>
<tr><td colspan="6">-</td></tr>
<tr><td colspan="2">2.70</td><td colspan="2">1.69</td><td colspan="2">1.85</td></tr>
<tr><td rowspan="5">IV-a</td><td colspan="2">70 to 112</td><td colspan="2">112 to 138</td><td colspan="2">138 to 160</td><td rowspan="5">4.68
(temperature in the cascade condenser, 117 ˚C)</td><td rowspan="5">1.73</td></tr>
<tr><td colspan="3">R1234ze(Z)</td><td colspan="3">R365mfc</td></tr>
<tr><td colspan="3">3.09</td><td colspan="3">8.38</td></tr>
<tr><td colspan="2">2.96</td><td colspan="2">-</td><td colspan="2">10.79</td></tr>
<tr><td colspan="2">3.00</td><td colspan="2">1.80</td><td colspan="2">1.51</td></tr>
<tr><td rowspan="5">IV-b</td><td colspan="2">70 to 87</td><td colspan="2">87 to 126</td><td colspan="2">126 to 160</td><td rowspan="5">4.56
(temperature in the cascade condenser, 92 ˚C)</td><td rowspan="5">1.69</td></tr>
<tr><td colspan="3">R717</td><td colspan="3">R365mfc</td></tr>
<tr><td colspan="3">2.12</td><td colspan="3">6.19</td></tr>
<tr><td colspan="2">5.23</td><td colspan="2">-</td><td colspan="2">9.88</td></tr>
<tr><td colspan="2">1.69</td><td colspan="2">2.59</td><td colspan="2">1.93</td></tr>
</table>

* Transmission-end-efficiency of electric power generation is assumed as 0.37

below 3. This is a significant benefit of reducing the throttling loss in the expansion valves and the mechanical fatigue in the compressors. The reduction of the throttling loss is illustrated in Figure 5 (b) by the short line segments of 6-7, 10-11, and 14-1. Additionally, by utilizing the subcoolers, the irreversible loss of heat transfer is reduced. In the extraction cycle, the extracted vapor rejects the heat once in the condenser and then converges with the refrigerant flow from the high-pressure side, which is somewhat flashed in the expansion valve. Thus, the internal energy of the refrigerant flow is transferred to the compressed water as much as possible, rather than wasted in the expansion valve. The reduced irreversible loss is illustrated in Figure 5 (b) by the line indicating the compressed water temperature bending up to the refrigerant temperature of the line segments 4-7-8-9-10 and 3-11-12-13-14. Comparing the overall COP between case III-a and III-b, the COP of case III-a is slightly higher than the others. The critical temperature, where the theoretical COP and volumetric capacity are almost maximized, of R1234ze(Z) is closer to the target temperature of the outlet compressed water. Most likely, this makes the use of R1234ze(Z) advantageous in the cycle. In addition, as shown in Figure 7 (a) the reduction in the COP with changes in the operation conditions is moderate, which means that this cycle could achieve the designed stable performance. The above mentioned thermodynamic attraction is significant; nevertheless, there is still a sticking point for the development. These multiple stage cycles do not allow the individual control of each stage, which makes the cycle control very difficult. To solve this problem partially, a cascade cycle is suggested.

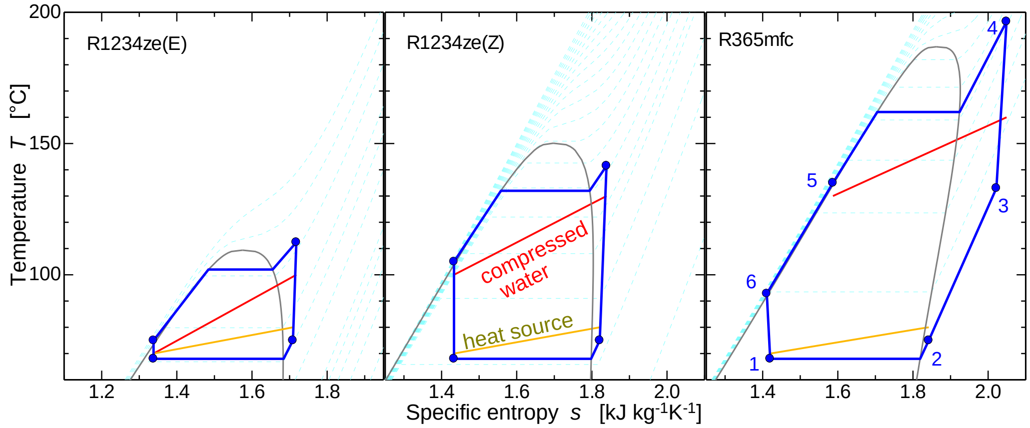

Figure 4: State of the cycle: case I with R1234ze(E), R1234ze(E), and R365mfc

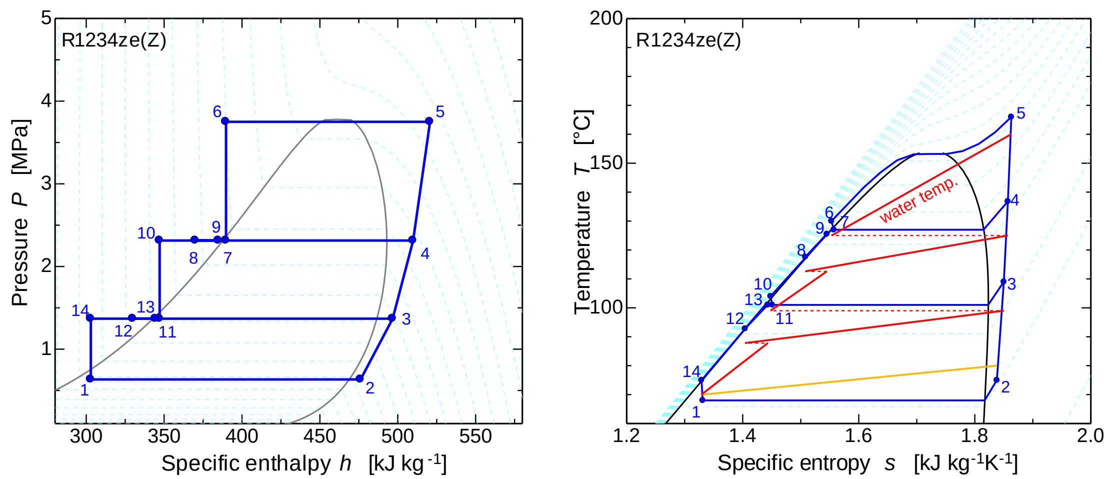

(a) *P-h* diagram (b) *T-s* diagram

Figure 5: State of the cycle: case III-a with R1234ze(Z)

For the cascade cycle case IV, the states of the low temperature side and the high temperature side are drawn by the dashed and solid lines in Figure 6. The irreversible loss due to the heat transfer is additionally generated in the cascade condenser, as illustrated by the area in between the solid line 6-7 and the dashed line 3-4. In consequence of the heat transfer loss, at the condensing temperature in the cascade condenser of 117 °C, the overall COP of the cascade cycle, case IV-a, applying R1234ze(Z) for the low side and R365mfc, is 4.68, which is somewhat lower than that of the multiple stage extraction cycles. As shown in Figure 7 (b), the overall COP of case IV decreases more than that of case III-a. The heat transfer loss in the cascade condenser can be increased according to the operation conditions, which does not occur in case III-a. Thus, the overall COP can be decreased considerably. Nevertheless, individual control is necessary for the high and low side stages. The cascade cycle brings some other practical benefits. For instance, the individual start and refrigerant selection of the low side stage can protect the compressors from the "liquid back" at the cold start. The lubricant oil can be selected for the particular temperature range of each stage. In addition, if a refrigerant possessing large volumetric capacity is used for the low side stage, then the downsizing of the compressor and some other parts of the heat pump can be allowed. Case IV-b is a cascade cycle applying R717 (i.e., ammonia) for the low stage side instead of R1234ze(Z), as listed in Table 3. The volumetric capacity of R717 at the low side stage is 5.23, which is 1.76 times that of the R1234ze(Z). This allows the drastic downsizing of the heat pumping unit and most likely the reduction in the irreversible loss by the pressure drop. Although the calculation result suggests slightly lower overall COP with R717 than with R1234ze(Z), the reversal pattern of the COP is possible in reality.

3.5 Effects of the compressor and heat exchanger performance on the COP

Table 4 shows the effect of the compressor efficiency and the heat exchanger size on the overall COP to set the lowest limit of development for these components. The variation in the overall COP of cases II, III-a, and IV-a is

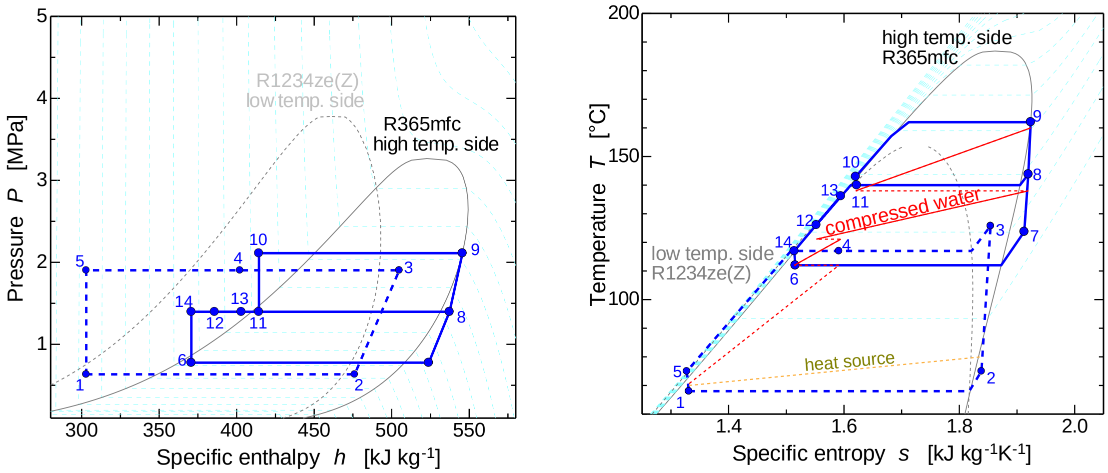

(a) *P-h* diagram (b) *T-s* diagram

Figure 6: State of the cycle: case IV-a with R1234ze(Z) and R365mfc

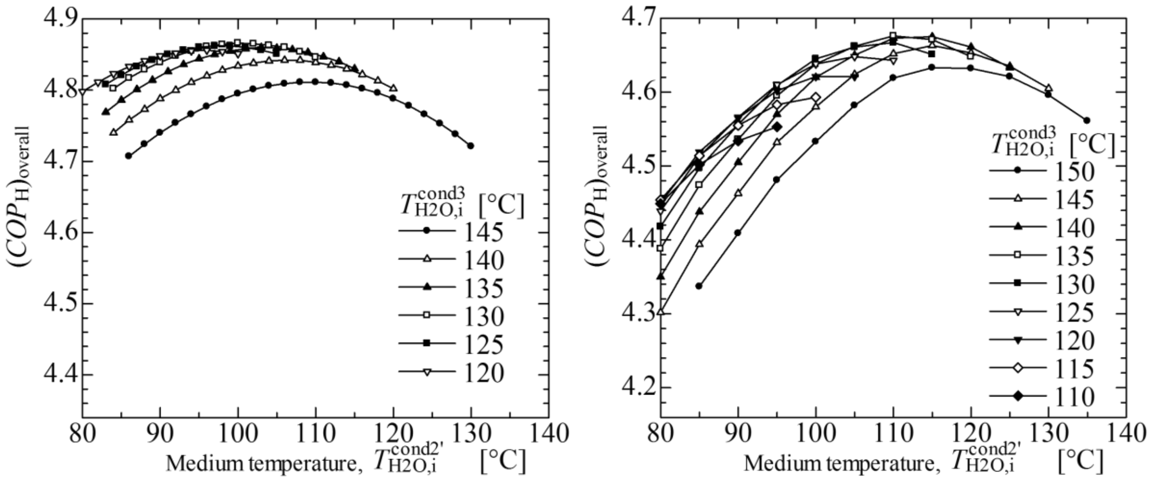

(a) case III-a (b) case IV-a

Figure 7: Variation in the overall COP against the change in the operation conditions

listed in Table 4. The conditions are gradually changed in the following steps. First, lowering the isentropic compression efficiency from 0.92 to 0.85, and 0.80, respectively, equivalent to the overall efficiency of the compressor of 0.70, 0.65, and 0.61. Second, enlarging the pinch temperature differences in the condenser and evaporator from 2 to 5, and 8 K. Similarly, at the condenser outlet, the temperature difference is increased from 5 to 8 K. With the first change in the isentropic compression efficiency, the overall COP decreases approximately 10%. With the enlarged temperature difference in the heat exchangers, the COP decreases approximately from 14 to 20%. The reason why the COP of case IV-a decreases more severely than the others is simply that many more heat exchangers are built into the cycle of case IV. Likewise, the COP decreases along with the gradually adverse conditions, and the primary energy efficiency decreases as well. At the worst conditions, the primary energy efficiencies are 1.38 to 1.51, still in excess of the criteria 1.0. Thus, once the assumed limit of development was achieved for a compressor and heat exchanger, these high-temperature heat pumps became advantageous over combustion boilers in terms of the energy consumption.

3.6 Effects of the heat recovery rate on the COP

Another major concern in the feasibility assessment is the balance of the waste heat amount and the heating load of the heat pumps. Ideally, if 100% of the waste heat was recovered, the heat pump systems could circulate the heat in a system perfectly, and other heating systems would be technically unnecessary. After complete removal of the waste heat, the heat source temperature is supposed to return to that of the ambient. Thus, the system has to raise the temperature from the ambient temperature to the target usage temperature that is, the net temperature lift. Further,

Table 4: Effects of the compressor efficiency and heat exchanger size (parenthesized percentages are relative COPs compared to the initial COPs).

		initial → → → → → adverse condition				
conditions	η_s	0.92	0.85	0.80	→	→
	η_{mech}	0.85	→	→	→	→
	η_{motor}	0.90	→	→	→	→
	η_{compr}	0.70	0.65	0.61	→	→
	ΔT_i^{EVAP}	2.0 K	→	→	5.0 K	8.0 K
	ΔT_i^{COND}	2.0 K	→	→	5.0 K	8.0 K
	ΔT_o^{COND}	5.0 K	→	→	→	8.0 K
$(COP_H)_{overall}$	case II	4.83 (100%)	4.64 (94%)	4.32 (89%)	4.25 (88%)	4.08 (84%)
	case III-a	4.94 (100%)	4.62 (96%)	4.39 (91%)	4.34 (90%)	4.14 (86%)
	case IV-a	4.68 (100%)	4.39 (94%)	4.18 (89%)	3.99 (85%)	3.74 (80%)
η_{pe}	case II	1.79	1.72	1.60	1.57	1.51
	case III-a	1.83	1.71	1.62	1.61	1.53
	case IV-a	1.73	1.62	1.55	1.48	1.38

Table 5: Effects of the temperature distribution in the heat source fluid (parenthesized percentages are relative values to the initial COPs).

		high → initial → → → → →→low				
conditions	$T_{src,i}$→ $T_{src,o}$	80→ 75 °C	80→ 70 °C	80→ 65 °C	80→ 60 °C	80→ 55 °C
	ΔT_{src}	5 K	10 K	15 K	20 K	25 K
$(COP_H)_{overall}$	case II	5.25 (109%)	4.83 (100%)	4.47 (92%)	4.15 (86%)	3.87 (80%)
	case III-a	5.40 (109%)	4.94 (100%)	4.54 (92%)	4.20 (85%)	3.92 (79%)
	case IV-a	5.06 (108%)	4.68 (100%)	4.34 (93%)	4.04 (86%)	3.77 (81%)
η_{pe}	case II	1.94	1.79	1.65	1.54	1.43
	case III-a	2.00	1.83	1.68	1.55	1.45
	case IV-a	1.87	1.73	1.61	1.50	1.40

the gross temperature lift, counting the driving temperature, is even greater. The large temperature lift leads almost directly to a decrease in the COP. There is a certain criterion of the heat-pump type heat recovery system to maintain a reasonable COP. To set the criteria of recovery amount, i.e., the heating capacity of the heat pump system, the change in the COP is simulated while varying the outlet temperature of the heat source fluid.

Table 5 is the calculation results of the COP and the primary energy efficiency of cases II, III-a, and IV-a. The parenthesized percentages are the values relative to the COP at the initial conditions specified in Table 2. When the outlet temperature of the heat source fluid in the evaporator is 75 °C, the waste heat is relatively abundant compared to the recovery and temperature change of the heat source fluid over the evaporator of 80 °C, which is only 5 K. The overall COP is from 8 to 9 % higher than that at the initial conditions. When the outlet temperature is 55 °C, the temperature change of the heat source fluid is 25 K, which is 2.5 times that of the initial conditions. The COP decreases to 3.77, which is 80 % of the COP at the initial conditions; nevertheless, the primary energy efficiency is 1.4, still above the criteria of 1.0. The amount of waste heat strongly depends on the environment where the systems are installed; therefore, there is preliminary estimate of the balance between the wasted and recovered heat. The above preliminary survey suggests that, under the conditions where the heat source temperature after usage is maintained above 55 K, heat recovery system of high-temperature applications are beneficial for the reduction of energy consumption.

4. CONCLUSIONS

An exploratory thermodynamic assessment of heat pump-type heat recovery systems using environmentally friendly refrigerants has been conducted. The coefficient of performance (COP) of four cycle configurations used to raise the temperature of compressed water up to 160 °C with a waste heat source of 80 °C were compared for the selected refrigerants R717, R365mfc, R1234ze(E), and R1234ze(Z). A multiple-stage “extraction” cycle drastically reduces the throttling loss in the expansion valve and the exergy loss in the condensers and consequently achieves the highest overall COP among the calculated cases, with refrigerant R1234ze(Z) having a critical temperature approximately equal to the target outlet water temperature. A cascade cycle using R1234ze(Z) and R365mfc results in a relatively high COP and also provides many practical benefits, such as the varied combination of refrigerants and lubricant oils and the prevention of the liquid-back caused by a cold start. At a compressor efficiency of 0.7 and an approach temperature difference in the heat exchangers of 2 K, the calculated overall COP ranges from 4.3 to 4.94. This corresponds to a primary energy efficiency of 1.62 to 1.83 when the transmission-end-efficiency of electric power generation is 0.37. Even with a compressor efficiency of 0.61 and an approach temperature of 8 K, the primary energy efficiency is greater than 1.3. As described above, the thermodynamic assessment demonstrated the potential of high-temperature heat pumps to recover waste heat as promising systems to reduce the primary energy consumption for industrial applications.

NOMENCLATURE

COP	coefficient of performance	(-)
P	pressure	(Pa)
Q	heat transfer rate	(W)
SC	degree of subcool	(K)
SH	degree of superheat	(K)
T	temperature	(°C)
VC	volumetric capacity	(J m^{-3})
W	work or input energy	(W)
h	specific enthalpy	(J kg^{-1})
m	mass flow rate	(kg s^{-1})
s	entropy	(J $kg^{-1}K^{-1}$)
η_{compr}	compressor efficiency	(-)
η_{mech}	mechanical efficiency	(-)
η_{motor}	motor efficiency	(-)
η_{pe}	primary energy efficiency	(-)
η_{s}	isentropic efficiency	(-)
ρ	density	(kg m^{-3})

Subscripts/Superscripts

compr	compressor
GC	gas cooler
H	heating
cond	condenser
SC	subcooler
evap	evaporator
V	vapor
r	refrigerant
H2O	compressed water (heat media)
src	heat source (waste heat)
IH	internal heat exchanger
i	inlet
o	outlet
overall	overall

REFERENCES

ASHRAE STANDARD, Designation and safety classification of refrigerants, ANSI/ASHRAE Standard 34-2007, 2008.

Akasaka, R., Higashi, Y., Koyama, S., 2013, A fundamental equation of state for low GWP refrigerant HFO-1234ze(Z), *Proc. 4th IIR Conference on Thermophysical Properties and Transfer Processes of Refrigerants*, Delft, The Netherlands, Paper No. TP-052.

Brown, J. S., Zilio, C., Cavallini, A., 2009, The fluorinated olefin R-1234ze(Z) as a high-temperature heat pumping refrigerant. Int. J. Refrig., vol. 32, 1412-1422.

Fleming, A.K., 1978, Refrigeration demands for meat processing, *Int. J. Refrig*., vol. 1, no. 4: p. 217-221.

Jakobs, R., Cibis, D., Laue, H. J., 2010, Status and outlook: Industrial heat pumps, Proc. International Refrigeration and Air Conditioning Conference at Purdue, Ray W. Herrick Laboratories, Paper no. 2282.

Kew, P.A., 1982. Heat pumps for industrial waste heat recovery – a summary of required technical and economic criteria. Heat Recovery System, vol. 2, no. 3, p. 283-296.

Koyama, S., Higashi, T., Miyara, A., Akasaka, R., 2013, JSRAE Risk Assessment of Mildly Flammable Refrigerants-2012 Progress Report, pp. 29-34.

Lemmon, E.W., Huber, M.L., McLinden, M.O., 2013, Reference Fluid Thermodynamic and Transport Properties - REFPROP Ver. 9.1, National Institute of Standards and Technology, Boulder, CO, USA.

Pearson, S.F., 1999, Ammonia refrigeration systems, *ASHRAE Journal*, vol. 41, no. 3, ProQuest Central: p. 24-29.

Solomon, S., Qin, D., Manning, M., Chen, Z., Marquis, M., 2007, IPCC 2007 Annual Report 4th Climate Change 2007 - The Physical Science Basis, 210-216.

U.S. Department of Energy, 2003, Industrial Heat Pumps for Steam and Fuel Savings, http://www1. eere.energy.gov /manufacturing/tech_assistance/pdfs/heatpump.pdf, pp. 1-15, (2003)

U.S. Department of Energy, 2008, Waste Heat Recovery: Technology and Opportunities in U.S. Industry, https:// www1.eere.energy.gov/manufacturing/intensiveprocesses/pdfs/waste_heat_recovery.pdf, pp.12-24.

ACKNOWLEDGMENTS

The present study is sponsored by the project on "Development on High Efficient and Non-Freon Air Conditioning System" of New Energy and Industrial Technology Development Organization (NEDO), Japan.